Brazilian Journal of Chemical Engineering

ISSN 0104-6632
Printed in Brazil
www.abeq.org.br/bjche

Vol. 24, No. 02, pp. 249 - 257, April - June, 2007

A STUDY OF TiAlN COATINGS PREPARED BY RF CO-SPUTTERING

L. García-González[1], M. G. Garnica-Romo[2*], J. Hernández-Torres[3] and F. J. Espinoza-Beltrán[4]

[1]Centro de Investigación en Micro y Nanotecnología,
Universidad Veracruzana, Boca del Río - Veracruz, México.
[2]Facultad de Ingeniería Mecánica, Universidad Michoacana de San Nicolás de Hidalgo,
Santiago Tapia 403, Col. Centro, C.P. 58000, Morelia - Mich., México.
E-mail: gromar05@yahoo.com.mx
[3]Universidad del Papaloapan, Campus Loma Bonita, Loma Bonita - Oaxaca, México.
[4]Centro de Investigación y de Estudios Avanzados del IPN,
Unidad Querétaro, Qro., México.

(Received: September 12, 2005 ; Accepted: January 25, 2007)

Abstract - Using the reactive magnetron rf co-sputtering technique and a Ti target partially covered with a small Al plate, TiAlN coatings were made on c-Si in a reactive atmosphere of nitrogen and argon. Coatings were deposited on substrates at 22°C and at 150°C. The substrate temperature notably affected the thickness, crystalline grain size, and hardness of the coatings. We analyzed the dependence of both structure and crystalline grain sizes on substrate temperature and the chemical composition of the coatings. The structural properties and the chemical composition were obtained by means of XRD and EDS techniques. High aluminum content was found in the coatings for the samples grown at the lower substrate temperature when samples were measured by electron dispersive spectroscopy technique. Atomic force microscopy measurements showed a surface morphology dependent on the nitrogen content. Scanning electron microscopy measurements showed a clear pyramidal microstructure of TiAlN coatings grown at 22°C, while the microstructure of those grown at a substrate temperature of 150°C were not well defined.
Keywords: Amorphous films; Reactive sputtering; TiAlN.

INTRODUCTION

Coatings of titanium nitride grown using the physical vapor deposition technique are of considerable interest for applications such as industrial tool coatings, since they extend the life of cutting and forming tools due to their outstanding mechanical properties. They are very hard and resistant to wear and corrosion, produce little friction, and have good resistance at high temperatures (Cunha et al., 1999; Wang et al., 1999). Their electrical conductivity also makes them an interesting material for microelectronic applications (Price et al., 1993; Hedge et al., 1993), and the intrinsic biocompatibility of TiN makes it a stable material for orthopedic implants, where it is mainly used to cover the head of knee prostheses (Dearnley, 1999; Piscanec et al., 2004). These coatings are also used as diffusion barriers in many semiconductors, and their brilliant gold color also makes them attractive for decorative applications (Harju et al., 1999). For PVD TiN layers with thickness of a few nanometers, a crystallographic texture is usually observable. The crystallographic orientation, typically either (111) or (002), depends on the PVD process parameters (temperature, bias voltage,

*To whom correspondence should be addressed

ionymetal flux ratio, etc.), nature of the substrate, and film thickness (Kodambaka et al., 2003; Chun et al., 2001; Oh and Je, 1993).

Adding aluminum to the TiN phase generally gives a polar interphase resulting in metallic or covalent bonding (Liu et al., 2004). Studies carried out in recent decades have revealed than TiAlN coatings have even better properties than do TiN coatings, and they have come to be considered the most promising and efficient hard coverings available today (Musil and Hrubý, 2000). This is why TiAlN coatings are widely used for cutting and forming tools, and they are particularly preferred for high velocity cutting processes, Lii (1998). Their outstanding characteristics, which include great resistance to oxidation at high temperatures and low thermal conductivity (Wu et al., 2000; Brogren et al., 2000) have led to their extensive use in integrated circuits as insulating barriers deposited on aluminum (Bhansali et al., 1990). These kinds of coatings are usually produced by sputtering (McIntyre et al., 1990; Shew et al., 1997), reactive electric arc evaporation (Rodríguez et al., 2002), or ionic implantation (Shiao et al., 2000). TiAlN is a metastable system with low thermal conductivity. These coatings can be used to form a dense protective layer with a high level of Al_2O_3 adhesion to the covered surface when this surface is heated, which prevents diffusion of oxygen into the covered material (Chakrabarti et al., 2002). The structure of (TiAl)N films depends a lot on the quantity of aluminum that is added to the compound. As greater amounts of aluminum are added, the color of the coating changes, turning dark gray, while the coating takes on the golden color of the TiN when less aluminum is added (Zeng et al., 2000).

The Warren-Averbach method is one of the methods currently used for measuring crystal grain size in powders and coatings from their X-ray diffraction pattern (McKeehan and Warren, 1953). With this method, the X-ray diffraction pattern peaks are corrected for the broadening of the diffraction lines, Lorentz dispersion, and diffraction due to the Cu-$K_{\alpha 2}$ line and then submitted to Fourier analysis. The Warren-Averbach method assumes that peak widening is due to the size distribution of the crystalline grains and to deformations due to internal stress in the lattice. The Pearson VII function was used for the line adjustments in the X-ray diffraction peaks.

In our present work, we studied the effect of two different substrate temperatures on the structure and mechanical properties of coatings obtained through reactive radiofrequency co-sputtering on silicon substrates with a (100) orientation. The Warren-Averbach method was used to adjust the diffraction peaks and derive information on the average crystalline grain size of the different phases present in our coatings. A previous study dealt with the mechanical properties of this system from the point of view of linkage formation (García-González et al., 2004).

EXPERIMENTAL PROCEDURE

TiAlN coatings were prepared by reactive radiofrequency co-sputtering and deposited on silicon substrates with an orientation of (100) and a Ti (99.995% pure) target. The coatings were prepared at two different substrate temperatures: room temperature and 150°C. A radiofrequency cathodic sputtering system with a model 5.0 Vacuum Products magnetron was used to make the deposits. This equipment achieved a residual vacuum of $2x10^{-6}$ Torr using both mechanical and diffusion pumps. In order to keep the equipment at a low temperature and thus make it possible to achieve a lower pressure more rapidly, the equipment was immersed in circulating water and a nitrogen trap was also used during the entire process of deposition. Once the vacuum was achieved, argon (Ar) was introduced into the chamber in order to achieve a pressure of 9 mTorr. A radiofrequency power of 180 W was used. Once the plasma was formed, pre-sputtering was done to clean the target, using an obturator to keep material coming off the target from reaching the substrate. Then the obturator was removed and Ti began to be deposited on the substrate, with the aim of forming a metallic bond between the substrate and the TiAlN coating, which improved the adherence of the nitride. After this, nitrogen was introduced and nitriding began. With the presence of the nitrogen in the chamber, the plasma changed color from purple to pink, but when there was too much nitrogen, the plasma takes on a reddish hue very quickly. The total pressure of both gases was 10 mTorr, and the growth period was typically 3 hours. Four sets of samples were produced and labeled M1, M2, M3, and M4. The M1 and M2 samples were made at room temperature and 150°C, respectively, using a tablet and M4. The M1 and M2 samples were made at room temperature and 150°C, respectively, using a tablet of Ti with an area of 5.07 cm^2 as the target. The M3 and M4 samples were also deposited using a tablet of Ti with an area of 5.07 cm^2 as the target but 20% of the effective area of this target was covered with an aluminum plate. The substrate was heated by placing an electrical resistor in contact with it and passing an electric current through it. The electrical current was automatically controlled by an electronic circuit. The details of the experiment are shown in Table 1.

The X-ray diffraction technique (XRD) was used to study the TiAlN coatings, using model DMAX/1200 Rigaku brand equipment and a Cu-Kα_1 line with a wavelength of 1.3406 Å. The morphological measurements as well as the Vickers hardness and fracture toughness measurements were done using a XL30 ESEM Philips scanning electron microscope, working in a high vacuum and in backscattered and secondary electron modes. This system is also equipped with an EDS-EDAX microprobe which makes it possible to obtain the chemical composition of the coatings. The surface morphology measurements were carried out using an atomic force microscope (AFM) (Dimension 3100 – Nanoscope IV from Digital Instruments). The Vickers hardness and fracture toughness of the coatings were measured with a Bruehler Micromet 2100 series micro-hardness tester with a Vickers indenter and loads of 0.098, 0.245, 0.49, 0.98, 1.96, and 2.94 N, with at least three indentations done per load.

Table 1: Parameters used for the TiN and (TiAl)N coatings on four silicon substrates.

Sample	Target (Effective area)	Substrate Temperature (°C)	Growth Time (Hr)
M1	100% Titanium	25	3
M2	100% Titanium	150	3
M3	80 % Titanium – 20% Aluminum	25	3
M4	80 % Titanium – 20% Aluminum	150	3

RESULTS AND DISCUSSION

The X-ray diffraction patterns for the samples grown on Ti targets are shown in Fig. 1 a). In the diffractogram for the M1 sample, shown at the bottom, fcc-TiN (JADE PDF-card # 38-1420) and hcp α-Ti (JADE PDF-card # 44-1294) crystalline phases can be identified (Inoue et al., 1995). It can also be seen that the relation of the intensity of the α-Ti and TiN diffraction peaks does not follow that which is found in the powders, which indicates that these crystals have preferential crystalline orientations. At a higher substrate temperature, in sample M2, only TiN phase peaks can be identified in the diffraction pattern. Since the M1 and M2 samples were deposited using pure Ti targets, only α-Ti and/or TiN phases can be expected. The SEM-EDS chemical composition results indicate that the M1 and M2 samples have about 50% atomic Ti and N (see Table 2 below). The higher substrate temperature appears to inhibit the formation of α-Ti crystals, favoring formation of the TiN phase. This behavior can be explained by extrapolating the equilibrium phase diagram of the binary Ti-N system to 150°C, which indicates that for atomic proportions of about 50:50% N:Ti, the most stable phase is TiN for temperatures of 500°C and above (Edenhofer et al., 1987). The Waren-Averbach model (McKeehan and Warren, 1953) was applied to estimate the average grain size of the crystals in both diffractograms. The grain size for the M1 sample was about 4.6 ± 0.6 nm (TiN) and 14.1 ± 3.9 nm (α-Ti). In the M2 sample the TiN grains had an average size of 7.2 ± 1.1 nm. The WinFit version 1.2.1 computer program (Program WinFit ver. 1.2.1, S. Krumm, Institut für Geologie Schlossgarten 5, 91054 Erlangen) was used for these calculations, in which Pearson VII functions were used to eliminate the contribution of the Cu-$K_{\alpha 2}$ line and background, as well as to correct for instrument expansion.

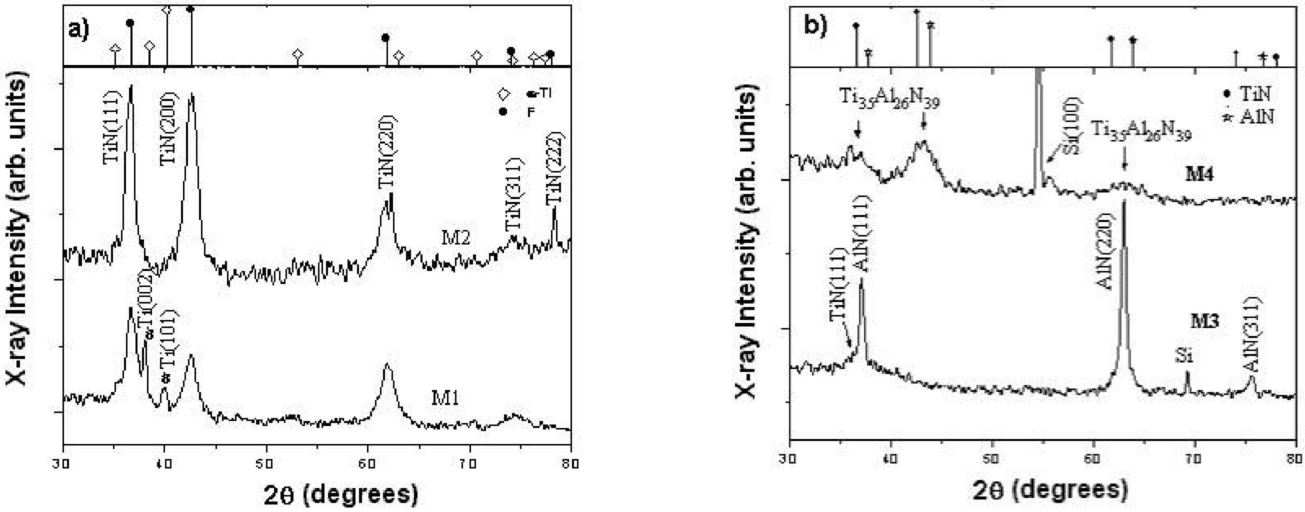

Figure 1: X-ray diffraction patterns in the 2θ range from 30 to 80° for the samples: a) M1 and M2; b) M3 and M4.

The diffractograms for the M3 and M4 samples, which were deposited on a Ti target with a small amount of aluminum adhered to the center of the target, are shown in Fig. 1 b). The M3 sample shows the characteristic peaks of the (111), (220), and (311) AlN phase, slightly shifted toward 2θ values (greater interplanar distances) that were lower than the reference positions (JADE PDF-card # 25-1495). Intrinsic stress, which appears during the process of depositing the coating, increases the difference between the crystalline atomic planes parallel to the surface of the sample. A wide, low intensity peaks which we associated with the presence of TiN nanocrystals, can be seen at the base of the peaks. When this diffraction pattern is adjusted using the Warren-Averbach model, it becomes clear that the M3 sample is a composite material composed of AlN and TiN phases, with a respective grain size of 14.3 ± 2.6 nm and 2.9 ± 0.3 nm. The diffractogram of the M3 sample, like that of the M1 and M2 samples, shows preferential crystalline orientations that prevent the appearance of AlN (200) and TiN (200) peaks, which are the most intense peaks found in powder samples. Finally, only narrow peaks due to the silicon substrate are seen in the X-ray diffraction pattern of the M4 sample, as well as three very wide, low-density peaks which more or less coincide with the (111), (200), and (220) X-ray diffraction peaks of both TiN and AlN. The proximity of the positions of the diffraction peaks for the TiN and AlN crystals (both having a face-centered cubic structure, fcc) is due to the fact that their lattice constant values are similar: 4.24173 and 4.0450 Å, respectively. The application of the Warren-Averbach model indicates that the material is composed of small crystals with an average grain size of 3.0 ± 0.3 nm. The material obtained evidenced an fcc-type cubic phase with a lattice constant of 4.194 Å, which is a value that falls between those of the TiN and AlN. This structure is a (Ti,Al)N ternary phase, whose composition, derived by SEM-EDS, is expressed by the formula $Ti_{35}Al_{26}N_{39}$.

The temperature of the substrate affected the thickness, structure, and hardness of the four samples. Evaluation of all the samples reveals that the higher temperature made the substrate harder and the coating thinner (Table 2). Vicker indentations with loads of 0.098, 0.245, 0.49, 0.98, 1.96, and 2.94 N were used to measure the hardness of the coatings on the Si substrate. At least three indentations were carried out for each load, and the diagonals of the impressions produced were measured by means of electron scanning microscopy. The hardness (H□) of the composite can be calculated from these diagonals using the following Eq. (1):

$$H_V = \frac{1.8544 * P}{d^2} \quad (1)$$

where P is the load applied (in Kgf) and d is the average length of the two diagonals (in mm). The range of loads applied makes it possible to generate a graph of hardness as a function of the relative penetration of the indenter. The behavior observed in all of the samples is expressed as a bell-shaped curve which describes the hardness of the coating-substrate composite for different relative microindentation depths, normalized for the thickness of the coating. An indentation-based hardness model was employed to eliminate the effect of the substrate and determine the hardness of the coating alone (Korsunsky et al. 1998), in accordance with the following approximation (Eq. 2):

$$H_c = H_s + \frac{H_f - H_s}{1 + k\beta^2} \qquad (2)$$

where H_c is the hardness of the composite; H_f and H_S are the hardness of the coating and the substrate, respectively; β is the relative depth (the depth of the indentation impression on the thickness of the coating); and k is a constant that depends on the material of which the coating and substrate are made.

Table 2: Results of different characterization techniques for all the samples.

Sample	Hardness (GPa)	Thickness (μm)	Grain size (nm)	N (at. %)	Al (at. %)	Ti (at. %)
M1	1.92 ± 1.22	1.603	4.6 ± 0.6 (TiN)	49.27	0	50.73
M2	9.92 ± 0.1	1.158	14.1 ± 3.9 (a-Ti)	48.17	0	51.83
M3	4.0 ± 4.7	1.74	7.2 ± 1.1 (TiN)	44.2	35.16	20.64
M4	10.83 ± 1.32	0.90	2.9 ± 0.3 (TiN)	39.46	25.97	34.57

The increase in hardness can be explained by considering both the values obtained for hardness, shown in Table 2, and the X-ray diffraction patterns of the samples shown in Fig. 1 a) and b). Due to the thinness of the samples, on the order of one micrometer, and the fact that the indentation system only allows a minimum load of 0.098 N, it was not possible to extend the range of loads applied. Because of these limitations it was not possible to obtain more precise adjustments for hardness vs. relative depth for the coatings studied. This is why there is a large margin of error in the results shown below. In the first case, the hardness of the samples increases from 1.92 ± 1.22 (for M1) to 9.92 ± 0.1 GPa (for M2) when the temperature is raised from room temperature to 150°C. This increase is due to the disappearance of the α-Ti phase; only TiN is found in the sample with the higher substrate temperature. TiN typically has a hardness of about 20.6 GPa (Ohring, 1992), which is a much higher value than that for Ti, with only 2.5 GPa. In the second case, the change in substrate temperature led to an increase in hardness values from 4.0 ± 4.64 GPa for the sample grown at 25°C (M3) to 10.83 ± 1.32 GPa for the sample grown at 150°C (M4). AlN and TiN phases were found in the M3 sample; the hardness of AlN is 11.8 GPa (Ohring, 1992), that is to say, less than that of TiN. When a temperature of 150°C was applied, these two phases disappeared, and only one ternary phase is present, with very small grains that are harder than those in the M3 sample. The substrate temperature also affected the thickness of the samples: the samples grown at the higher temperature were thinner. Electron scanning microscopy images of the indentation impressions produced by a load of 0.49 N are shown in Fig. 2 for (a) M1, (b) M2, (c) M3, and (d) M4. A fracture starting from the vertices of the impression left by the Vicker indenter can be seen in all the samples. Since most of the samples do not comply with minimal thickness requirements (Karimi et al., 2002; Scharf et al., 1997) we will only deal here with their fracture toughness in a qualitative sense. All the cracks are collinear with the diagonals of the impressions made by the hardness tester with the Vickers indenter, which are measured from the center of the Vickers impression. These kinds of cracks are known as primary "half-penny" fractures. With loads greater than 0.49 N, secondary cracks also appear, and these were classified as "lateral" fractures since they appear around the Vickers impression. Fracture toughness of hard coatings was measured by ICL (indentation crack length) using the equation proposed by Lawn and Evans (Lawn et al., 1980). The samples grown at substrate temperatures of 150°C were more fragile than those grown at room temperature, as can be seen in the images in Fig. 2. The M1 sample had little adherence to the substrate, as can be seen in 2(a): the coating is beginning to come off the substrate, and this becomes more evident with the application of heavier loads. Higher temperature improved the adherence of the coating, as can be seen in image 2(b). Images 2(c) and 2(d) also show that the adherence of the coating improved at the higher substrate temperature.

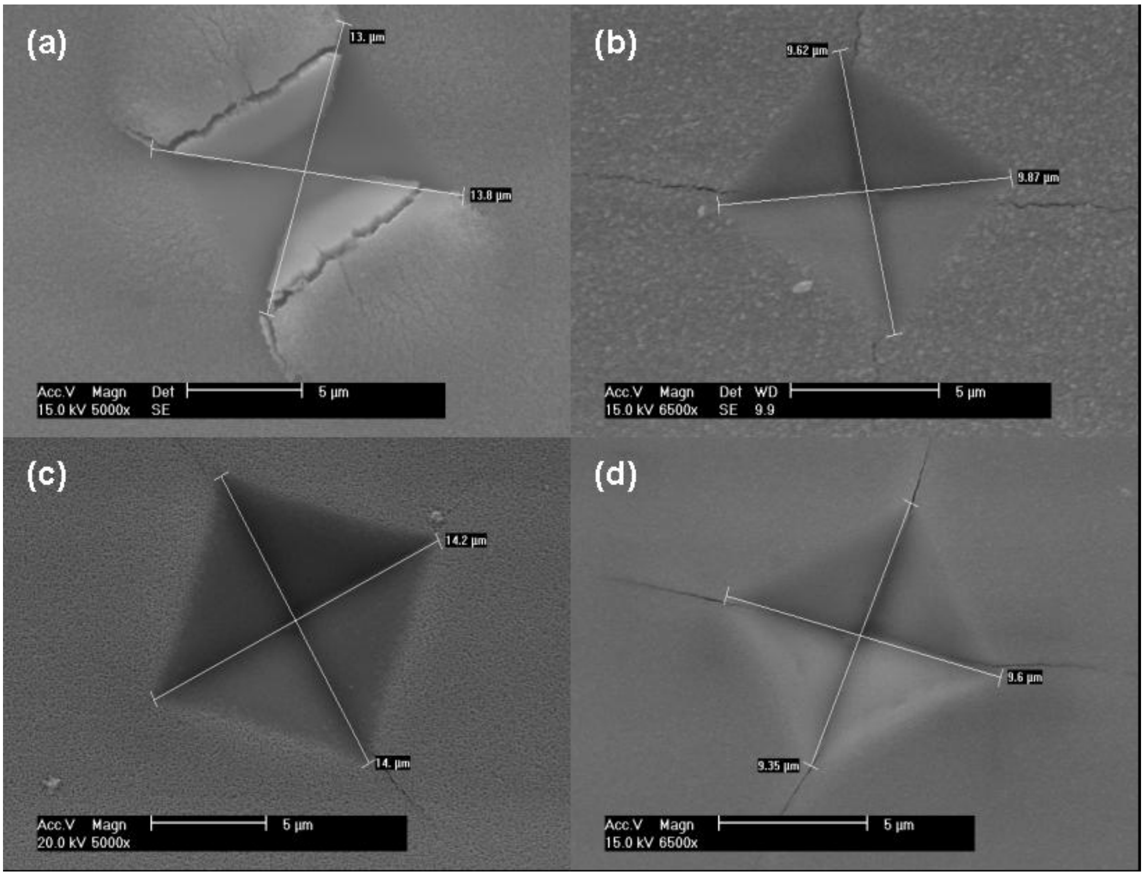

Figure 2: Electron scanning microscopy images showing the indentation impressions produced with a load of 0.49 N in the samples: (a) M1, (b) M2, (c) M3, and (d) M4.

In Fig. 3 we can see photographs of the microstructure of the samples from a scanning electron microscope, magnified 35,000 times for (a) M1 and (b) M2, and 65,000 for (c) M3 and (d) M4. Image 3(a), corresponding to a mixture of TiN and α-Ti, shows a surface with small, pyramid-shaped grains with sizes on the order of a tenth of a micrometer. A few irregularly shaped grains of a slightly lighter color are also observed. The former grains are agglomerates of TiN crystals with a preferential orientation of (111), and the larger, irregularly shaped grains are aggregates of α-Ti without preferential orientation. Image 3(b) corresponds to TiN and shows rectangular, prism-shaped grains that are several tenths of a micrometer in size. The X-ray diffraction results indicate that these prisms are agglomerates of TiN crystals with a random crystallographic orientation and a slight tendency toward a crystalline orientation of (111). In image 3(c), agglomerates of pyramidal structures can be seen that correspond to AlN crystals oriented in the (111) direction. A smaller proportion of darker, irregular structures can also be seen; these may correspond to the amorphous or nanocrystalline phase of TiN, according to the results shown in Fig. 1 b). Image 3(d) is a micrograph of the $Ti_{35}Al_{26}N_{39}$ ternary phase, where it can be seen that the higher temperature broke up the agglomerates of small pyramids in the M3 sample, which was completely transformed into an amorphous phase with very small grains that can just barely be perceived.

The surface topography images for the samples (a) M1, (b) M2, (c) M3, and (d) M4 are shown in Fig. 4 for an area of 5.0 x 5.0 μm^2 and a scanning velocity of 0.5 Hz. The vertical scale is the same for all the images. The values for quadratic roughness decline with increased temperature and this corroborates the grain size results obtained by the Warren-Averbach method.

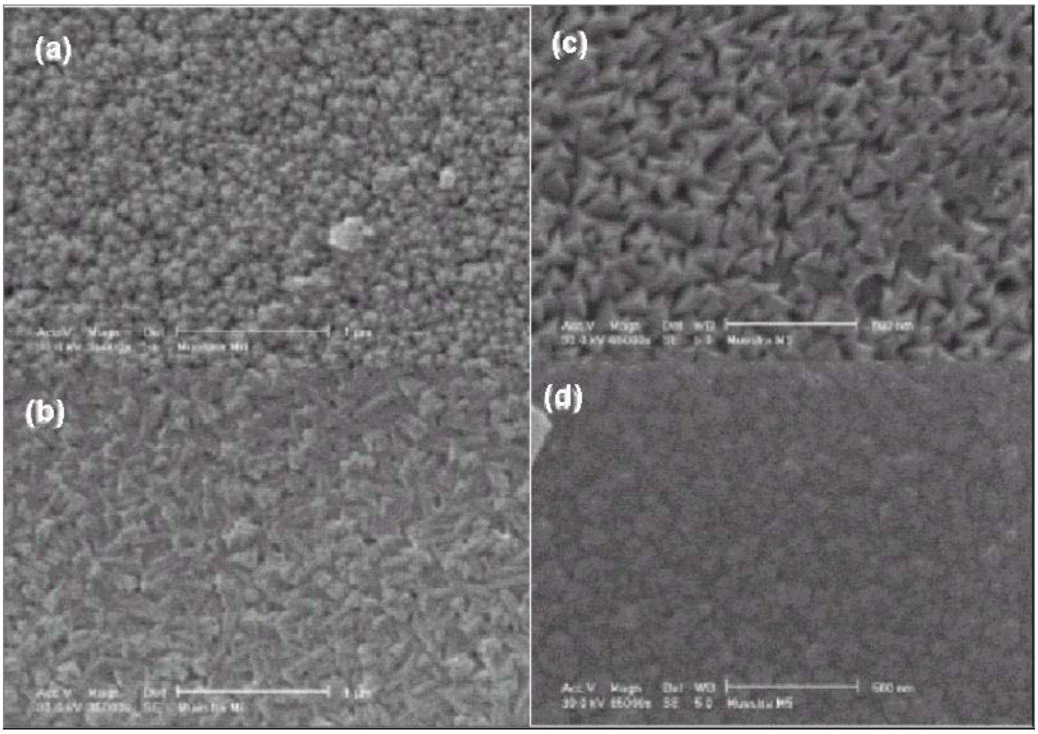

Figure 3: Electron scanning microscopy images of the surface of the samples, with a magnification of 35,000 for (a) M1and (b) M2 and a magnification of 65,000 for (c) M3 and (d) M4.

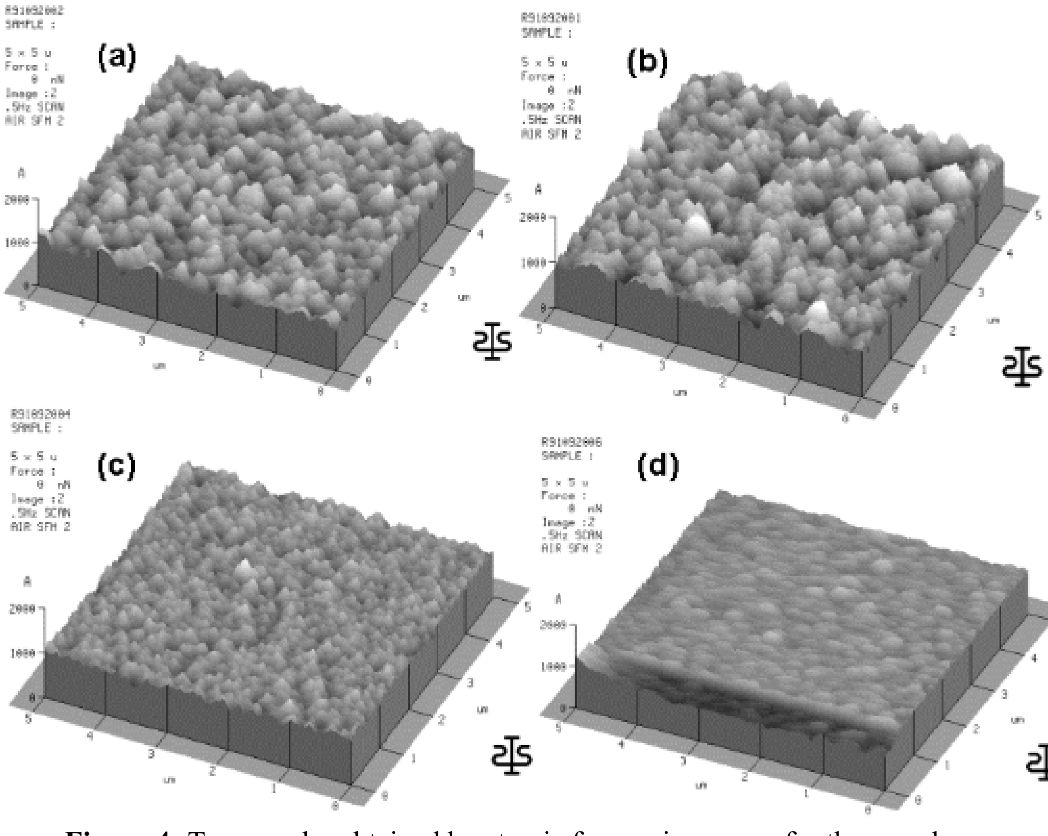

Figure 4: Topography obtained by atomic force microscopy for the samples: (a) M1, (b) M2, (c) M3, and (d) M4.

CONCLUSIONS

The effect of substrate temperature on the mechanical and structural properties of (Ti,Al)N coatings produced by reactive radiofrequency co-sputtering was studied. In the absence of aluminum, increased temperature prevents the formation of α-Ti crystals and favors the formation of the TiN phase, which considerably increases the hardness of the coatings. When aluminum is added to the coatings, the hardness of the coatings is improved due to the formation of a composite material, and a ternary phase appears at the higher substrate temperature which is harder than all the other samples. The Warren-Averbach method was used to analyze the experimental x-ray diffraction lines, employing the theoretical line profile provided by the pseudo-Voight function. From that analysis the crystalline grain size distributions and the average grain sizes were obtained. Higher temperature resulted in greater hardness, lower fracture toughness, and thinner coatings. The real hardness value of the coatings, eliminating the substrate effect, was estimated using the indentation-based hardness model.

ACKNOWLEDGEMENTS

This work received the finnancial support of the Consejo Nacional de Ciencia y Tecnología (CONACYT) through Project G33178-U and the Consejo de Ciencia y Tecnología del Estado de Querétaro. The authors would also like to thank the following assistants for their help: Ing. Pedro García Jiménez, Ing. José Eleazar Urbina Álvarez, Ing. Martín Adelaido Hernández Landaverde, as well as Jairo A. Cardona Bedolla, MS (physics).

REFERENCES

Bhansali, A. S., Sinclair, R., Morgan, A.E. (1990). A Thermodynamic Approach for Interpreting Metallization Layer Stability and Thin Film Reactions Involving Four Elements: Application to Integrated Circuit Contact Metallurgy. J. Appl. Phys., 68, 1043.

Brogren, M., Harding, G. L., Karmhag, R., Ribbing, C. G., Niklasson, G. A., Stenmark, L. (2000). Titanium-Aluminum-Nitride Coatings for Satellite Temperature Control. Thin Solid Film, 370, 268.

Chakrabarti, K., Jeong, J. J., Hwang, S. K., Yoo, Y. C., Lee, C. M. (2002). Effects of Nitrogen Flow Rates on the Growth Morphology of TiAIN Films Prepared by an rf-Reactive Sputtering Technique. Thin Solid Films, 406, 159.

Chun, J-S., Desjardins, P., Lavoie, C., Shin, C-S., Cabral, Jr. C., Petrov, I. (2001). Interfacial reactions in Epitaxial Al/TiN (111) Model Diffusion Barriers: Formation of an Impervious Self-Limited Wurtzite-Structure AIN (0001) Blocking Layer. J. Appl. Phys., 89, 7841.

Cunha, L., Andritschky, M., Rebouta, L., Pisehow, K. (1999). Corrosion of CrN and TiAIN Coatings in Chloride-Containing Atmospheres. Surf. Coat. Technol. 116, 1152.

Dearnley, P. A. (1999). A Review of Metallic, Ceramic and Surface-Treated Metals Used for Bearing Surfaces in Human Joint Replacements. P. I. Mech. Eng. H, 213, 107.

Edenhofer, B., Jacobs, M. H., Georges, J. N. (1987). International Seminar on Plasma Heat Treatment, 399-420.

García-González, L., Morales-Hernández, J., Bartolo-Pérez, J. P., Ceh-Soberanis, O., Muñoz-Saldaña, J., Espinoza-Beltrán, F. J. (2004). Estudio de Películas Amorfas de TiAIN Preparadas por Erosión Catódica Reactiva por Radiofrecuencias. Revista Mexicana de Física, 50 (3), 311.

Harju, E., Kivivuori, S., Korhonen, A. S. (1999). Formation of a Wear Resistant Non-Mettalic Protective Layer on PVD-Coated Cutting and Forming Tools. Surf. Coat. Technol,. 98, 112.

Hedge, R. I., Fiordalice, R. W., Travis, E. O., Tobin, P. J. (1993). Thin Film Properties of Low-Pressure Chemical Vapor Deposition TiN Barrier for Ultra-Large-Scale Integration Applications. J. Vac. Sci. Technol. B, 11, 1287 (1993).

Inoue, S., Ucihda, H., Takeshita, K., Koterazawa, K., Howsno, R. P. (1995). Preparation of Compositionally Gradient Ti-TiN Films by r.f. Reactive Sputtering. Thin Solid Film, 115, 261.

Karimi, A., Wang, Y., Cselle, T., Morstein, M. (2002). Fracture Mechanisms in Nanoscale Layered Hard Thin Films. Thin Solid Films, 420-421, 275.

Kodambaka, S., Chopp, D. L., Petrov, I., Greene, J. E. (2003). Coalescence Kinetics of Two Dimensional TiN Islands on Atomically Smooth TiN (0 0 1) and TiN (1 1 1) Terraces. Surf. Sci., L611, 540.

Korsunsky, A. M., McGurk, M. R., Bull, S. J., Page, T. F. (1998). On the Hardness of Coated Systems. Surf. Coat. Technol. 171, 99.

Lawn, B. R., Evans, A. G., Marschall, D. B. J. Am. Ceram. Soc., 63, 574 (1980).

Lii, D. F. (1998). The Effects of Aluminium Composition on the Mechanical Properties of Reactivity Sputtered TiAlN Films. J. Mater Sci. 33, 2137.

Liu, L. M., Wang, S. Q., Ye, H. Q. (2004). First Principles Study of Polar Al/TiN (1 1 1) Interfaces. Acta Mater., 52, 3681.

McIntyre, D., Greene, J. E., Hakansson, G., Sundgren, J. E., Munz, W. D. (1990). Oxidation of Metastable Single-Phase Polycrystalline $Ti_{0.5}A1_{0.5}N$ Films: Kinetics and Mechanism. J. Appl. Phys., 67, 1542.

McKeehan, M., Warren, B. E. (1953). X-ray Study of Cold Work in Thoriated Tungsten. J. Appl. Phys., 24, 52.

Musil, J., Hrubý, H. (2000). Superhard Nanocomposite $Ti_{1-x}Al_xN$ Films Prepared by Magnetron Sputtering. Thin Solid Film 104, 365.

Oh, U. C., Je, J. H. (1993). Effects of Strain Energy on the Preferred Orientation of TiN Thin Films. (1993). J. Appl. Phys., 74, 1692.

Ohring, M. (1992). Chapter 12: Mechanical Properties of Thin Films. The Materials Science of Thin Films. Academic Press, 552.

Piscanec, S., Colombi .L., Vesselli, E., Comelli, G., Sbaizero, O., Meriani, S., De Vita, A. (2004). Bioactivity of TiN-Coated Titanium Implants. Acta Mater., 52, 1237.

Price, J. B., Borland, J. O., Selbrede, S. (1993). Properties of Chemical-Vapor-Deposited Titanium Nitride. Thin Solid Films, 236, 311.

Rodríguez, R. J., García, J. A., Medrano, A., Rico, M., Sánchez, R., Martínez, R., Labrugère, C., Lahaye, M., Guette, A. (2002). Tribological Behaviour of Hard Coatings Deposited by Arc-Evaporation PVD. Vacuum, 67, 509.

Scharf, T. W., Deng, H., Barnard, J. A. (1997). Mechanical and Fracture Toughness Studies of Amorphous SiC-N Hard Coatings using Nanoidentation. J. Vac. Sci. Technol,. A, 15, 963.

Shew, B. Y., Huang, J. L., Lii, D. F. (1997). Effects of r.f. Bias and Nitrogen Flow Rates on the Reactive Sputtering of TiAlN Films. Thin Solid Films, 293, 212.

Shiao, M-H., Kao, S-A., Shieu, F-S. (2000). Effects of Processing Parameters on the Microstructure and Hardness of the Arc Ion-Plated TiN on a Type 304 Stainless Steel. Thin Solid Films, 375, 163.

Wang, D. Y., Li, Y-W., Chang, C-L., Ho, W-Y. (1999). Deposition of High Quality (Ti, Al)N Hard Coatings by Vacuum Arc Evaporation Process. Surf. Coat. Technol. 114, 109.

WinfFit V1.2, S. Krumm, Institut für Geologie Schlossgarten 5, 91054 Erlangen.

Wu, S. K., Lin, H. C., Liu, D. L. (2000). An Investigation of Unbalanced-Magnetron Sputtered TiAlN Films on SKH51 High-Speed Steel. (2000). Surf. Coat. Technol,. 124, 97.

Zeng, X. T., Zhang, S., Muramatsu, T. (2000). Comparison of Three Advanced Hard Coatings for Stamping Applications. Surf. Coat. Technol., 38, 124.